

## Advanced Biomaterials for Periodontal Tissue Regeneration

Arwa Daghreery<sup>a</sup> and Marco C. Bottino<sup>b,c,\*</sup>

<sup>a</sup> Department of Restorative Dental Sciences, School of Dentistry, Jazan University, Jazan, Kingdom of Saudi Arabia.

<sup>b</sup> Department of Biomedical Engineering, College of Engineering, University of Michigan, Ann Arbor, Michigan, United States.

<sup>c</sup> Department of Cariology, Restorative Sciences, and Endodontics, University of Michigan, School of Dentistry, Ann Arbor, Michigan, United States.

**\*Corresponding author:**

**Marco C. Bottino, DDS, MSc, PhD**

Associate Professor

University of Michigan School of Dentistry

Department of Cariology, Restorative Sciences, and Endodontics

1011 N. University (Faculty Commons, Room 3146), Ann Arbor, MI - 48109, USA.

Tel: +1-734.763.2206 Fax: +1-734.936.1597

E-mail address: [mbottino@umich.edu](mailto:mbottino@umich.edu) (Dr. Marco C. Bottino)

This is the author manuscript accepted for publication and has undergone full peer review but has not been through the copyediting, typesetting, pagination and proofreading process, which may lead to differences between this version and the Version of Record. Please cite this article as doi: [10.1002/dvg.23501](https://doi.org/10.1002/dvg.23501)

This article is protected by copyright. All rights reserved.

## **Summary**

The periodontium is a suitable target for regenerative intervention, since it does not functionally restore itself after disease. Importantly, the limited regeneration capacity of the periodontium could be improved with the development of novel biomaterials and therapeutic strategies. Of note, the regenerative potential of the periodontium depends not only on its tissue-specific architecture and function, but also on its ability to reconstruct distinct tissues and tissue interfaces, suggesting that the advancement of tissue engineering approaches can ultimately offer new perspectives to promote the organized reconstruction of soft and hard periodontal tissues. Here, we discuss material-based, biologically active cues, and the application of innovative biofabrication technologies to regenerate the multiple tissues that comprise the periodontium.

## **Keywords**

3D printing; Biofabrication; Biomaterials; Bioprinting; Infection; Periodontitis; Regeneration; Scaffolds

## 1. INTRODUCTION

Periodontal disease (PD) is one of the most destructive inflammatory oral disorders, affecting roughly 45% of the adult population in the United States (Eke et al., 2015). This chronic inflammatory disease is defined by the slow degradation and loss of alveolar bone and other periodontal tissues (*i.e.*, cementum, gingiva, and periodontal ligament) (Eke et al., 2015). If left untreated, PD triggers tissue destruction, resulting in tooth mobility and eventual tooth loss (Könönen et al., 2019). Traditional PD treatment focuses on eradicating infection and lowering inflammation to halt disease development. However, conventional approaches do not regenerate destroyed periodontal tissues (Liang et al., 2020). In particular, the clinical outcome is often a repair process, rather than complete restoration of the periodontium's function and architecture. Successful periodontal regeneration mandates alveolar bone reconstruction and the formation of periodontal ligament (PDL) fibers embedded in the newly formed cementum (Dangaria et al., 2011 and Dagherery et al., 2022).

Periodontal tissue regeneration has been achieved using various clinical procedures, such as guided tissue/bone regeneration (GTR/GBR) with or without bone grafts. However, the therapeutic benefits of these methods remain uncertain, and their regeneration potential is limited. The outcomes are measurable but insufficient to restore functional periodontal tissue after severe destructive disease (Aytac et al., 2021). Notably, over the last decade, materials- and regenerative-based approaches, including enamel matrix derivatives, growth factors, gene delivery, and cell transplantation in association with matrix-based scaffolds, have evolved with clinically promising potential (Bottino et al., 2012; Aytac et al., 2021). Synthetic and natural polymers and composite materials are the most frequently employed biomaterial strategies in periodontal tissue regeneration. Scaffolds for cementum and bone regeneration, for example, have been developed by combining inorganic and polymeric components, such as polylactic acid (PLA), polylactic-co-glycolic acid (PLGA), polycaprolactone (PCL), collagen, hydroxyapatite (HA), and tricalcium phosphate (TCP) (Bottino et al., 2012; Aytac et al., 2021).

Despite their promising potential, these biomaterials partially recapitulate the compositions and properties associated with native periodontal tissues. Remarkably, the periodontium is a bundle of tissues (*i.e.*, gingiva, alveolar bone, periodontal ligament, and cementum) that holds the tooth and protects the underlying

structures (**Figure 1**). Hence, regeneration of one or two periodontium elements is insufficient to restore functionality. To date, the majority of monophasic or biphasic biomaterial-based scaffolds have shown limited potency in regenerating complex multiphasic tissues (Dan et al., 2014; Yu et al., 2022). Thus, the regeneration of periodontium remains an elusive goal, despite recent advances in tissue engineering, making it seem excitingly close. Several challenges must be resolved to achieve clinically significant regeneration, including specificity to defect size, tissue compositions, and architectures. Moreover, the integration of multifunctional therapeutic cues to eradicate infection/inflammation and recruit stem/progenitor cells would provide a microenvironment conducive to cell proliferation, differentiation, and development of new tissue through consecutive steps (Bottino et al., 2012).

Collectively, this review offers an update on the latest advancement in periodontal regeneration employing tissue engineering and regenerative medicine. We focused on therapeutics and bioactive cues to aid in the regeneration of the periodontium. A specific emphasis is placed on engineering bioinspired material-based approaches with spatiotemporal regulation of multifunctional cues to support reliable periodontal reconstruction and effective clinical translation.

## **2. PERIODONTAL TISSUE DEVELOPMENT**

During tooth formation, the dental papilla gives rise to two main structures: odontoblasts and dental pulp, while the dental follicle develops into the periodontium's main components: cementum, periodontal ligament (PDL), and alveolar bone (Xiong et al., 2013). Periodontal tissues originate from dental follicles derived from the neural crest and develop alongside the tooth roots (Xiong et al., 2013).

Generally speaking, the dental follicle is a sac of loose ectomesenchyme-derived connective tissue that encloses an unerupted tooth (Yao et al., 2008). The dental follicle involves two main components: (a) the proper, well-defined band of groups of cells apposed to the dental papilla and the convex outer surface of the enamel organ, and (b) the perifollicular mesenchyme, which is a loosely defined population of cells surfacing from the developing trabeculae surrounding the tooth bud (Cho & Garant, 2000). These layers are separated by a poorly populated zone of loose connective tissue during tooth bud extirpation, forming a natural cleavage plane, whereas the perifollicular mesenchyme and the attached bony trabeculae mainly form tooth-supporting structures (Cho & Garant, 2000).

The periodontium comprises multiple tissues, consisting of gingiva, root-lining cementum, periodontal ligament (PDL), and alveolar bone that supports the teeth (Torabi & Soni, 2021). Histologically, the cervical root is often covered by acellular cementum, while the apical root is covered by thick cellular cementum comprising both fibrillar and afibrillar cementum. The PDL is a highly cellular structure rich with undifferentiated stem cells, blood vessels, and sensory nerve endings, which lie between the cementum and alveolar bone (**Figure 1**). The alveolar bone has a lamellar structure and a densely-rich periosteum containing osteoblasts, osteoclasts, arteries, and nerves.

When a tooth matures, the niche (microenvironment) necessary for forming tooth-supporting tissues diminishes, making it challenging to restore damaged/lost periodontium. Thus, efforts have been made to implement tissue engineering strategies and develop hierarchical architecture by replicating the highly specialized microenvironment to regenerate functional periodontal tissues. It is worth noting that many investigations in regenerative endodontics observed ectopic PDL-like tissue formation within the root canals, rather than pulp tissue regeneration (Wang et al., 2010; Yamauchi et al., 2011; Palma et al., 2017). This can be attributed to either apical papilla migration into the intra-pulpal space or an influx of PDL stem cells due to excessive instrumentation during the root canal treatment of immature or mature teeth. The lack of pulp-like or dentin-like tissue denotes the need for incorporating factors that support regenerative microenvironments and benefits stem/progenitor cell differentiation.

Periodontal tissue regeneration is a complex process that necessitates control of local infection and suppressing the inflammation to establish a healthy environment for regeneration. Moreover, when considering a tissue engineering strategy, two key factors must be considered: (a) a scaffold, including the appropriate selection of biomaterials and the scaffold's design, and (b) temporal release of antibacterial/anti-inflammatory medications and regulatory molecules, including bioactive cues, growth factors and the delivery of cells (Bottino et al., 2012; Liang et al., 2020). Furthermore, since the periodontium comprises different tissues, distinctive biological cues must be considered to direct the formation of each structure. Hence, to predictably regenerate soft (gingiva and periodontal ligament) and mineralized (alveolar bone and cementum) tissues, specialized zonal-specific attributes, *i.e.*, biological cues, stem cells, and tissue-specific guiding platforms, are fundamental (Pilipchuk et al., 2018; Yu et al., 2022).

### 3. PERIODONTAL TISSUE ENGINEERING

#### 3.1 Antibacterial and Anti-inflammatory Therapeutics

Several strategies have been used for localized drug delivery to ablate periodontal infection, such as polymeric strips, microspheres, antibiotic-laden hydrogels, or polymeric nanofibers (Friesen et al., 2002; Lee et al., 2008; Shahi et al., 2017; Ribeiro et al., 2020). In periodontal defects, antibiotic-laden polymeric scaffolds enclosing a combination of metronidazole (MET) and tetracycline (TCH) were able to ablate infection, while presenting defect-specific capacity to support the reconstruction of three-wall osseous defects in a rat model (**Figure 2A**) (Ferreira et al., 2021). Remarkably, the antibiotic-laden (MET/TCH) electrospun scaffolds acted as a framework for Bio-Oss<sup>®</sup> to foster new bone formation, while successfully reducing inflammatory cell infiltration over 6 weeks (**Figure 2A1-A2**) (Ferreira et al., 2021). These findings confirm that the incorporation of antibiotics within clinically translatable biodegradable scaffolds has the potential to eradicate infection and support the regeneration of lost tissues.

Given the unique anatomy and geometrical intricacy of tissue loss caused by periodontitis, the ability of injectable systems to flow freely into these highly complex structures is crucial for ensuring a complete and effective infection eradication (Ribeiro et al., 2020). A hybrid system of injectable hydrogels (GelMA)/ciprofloxacin [CIP]-complexed to beta-cyclodextrin [ $\beta$ -CD]) has been produced for infection ablation (Ribeiro et al., 2020). The presence of the CIP/ $\beta$ -CD complex and the GelMA's tunable degradation profile provided superior solubility enhancement of cell-friendly antibiotic doses with significant antimicrobial potential. The injectable hybrid system exemplifies an effective method to attenuate the growth of *Enterococcus faecalis*, a clinically relevant oral pathogen (Ribeiro et al., 2020).

In a recent study, an injectable thermoresponsive hydrogel containing bone morphogenetic protein-7 (BMP-7) and ornidazole (ORN) supported periodontal regeneration in dogs with Class III periodontal furcation defects due to BMP-7 release kinetics' cumulative effect and ORN's antibacterial action (Zang et al., 2019). Furthermore, a wide variety of electrospun fibrous scaffolds can be engineered with potent bone-forming molecules/compounds and antimicrobial action (e.g., zinc oxide, ZnO) as clinically relevant therapeutics (Nasajpour et al., 2018). Likewise, electrospun PCL fibers containing hydroxyapatite (HAp) particles and amoxicillin (AMX) provided antimicrobial action and enhanced mineral deposition (Furtos et al., 2017).

Alternatively, coaxial electrospinning can provide spatiotemporal release patterns of antimicrobial and osteogenic cues to initially eradicate infection and then support bone formation (He et al., 2017).

Composite membranes prepared using chitosan, polyvinyl alcohol, and hydroxyapatite containing meloxicam (a nonsteroidal anti-inflammatory drug) demonstrated substantial anti-inflammatory action, suggesting their potential use in periodontal therapy (Ngawhirunpat et al., 2009). Recently, bioprinted osteoblasts-laden alginate-based hydrogels containing diclofenac were used to manage inflammation and promote a healthy bone growth (Lin et al., 2018). The printed system improves the scaffold's drug retention and release properties and biocompatibility. While considerably reducing the inflammatory cytokine by macrophage, the bone cells establish their mineralization in a favorable microenvironment (Lin et al., 2018). Meanwhile, a novel immunomodulatory approach that targets periodontal tissue regeneration has recently been reported (Hu et al., 2018). The proposed method targets macrophages, which are vital in the activation and resolution of inflammation. It primarily allows for the transition of classically activated pro-inflammatory M1 into pro-healing M2 macrophages (Hu et al., 2018). Accordingly, the dynamic switch in the phenotype environment can be conditioned by releasing cytokines specific to the osteoimmunomodulatory strategy. For instance, a biomimetic microenvironment resembling the natural bone extracellular matrix (ECM) was synthesized using a microsphere that was self-assembled with heparin-modified gelatin nanofibers. Importantly, the incorporated Interleukin 4 (IL4), which possesses heparin-binding domains, provided a sustained cytokine release and efficiently suppressed inflammation, subsequently enhancing new bone formation *in vivo* (**Figure 2B**) (Hu et al., 2018). Altogether, opportunities associated with injectable therapeutics, nanofibrous scaffolds, or bioprinting techniques offer prospects to eradicate infection, suppress inflammation, and hasten periodontal tissue regeneration.

### **3.2 Cues for Alveolar Bone Formation**

Over the years, alveolar bone repair has mainly relied on grafting material derived from autograft, allograft, or synthetic substitutes. However, this strategy raises concerns about the need for several surgeries, related morbidity, and potentially catastrophic consequences of infection in the operated area (Bottino et al., 2012). Furthermore, bone grafts may fail to conform to the defect's shape and size and sustain physiological function (Aytac et al., 2021).

Guided tissue regeneration (GTR) and guided bone regeneration (GBR) have consistently been the vital means of managing and clinically treating periodontitis-caused tissue degradation (Bottino et al., 2012). GTR/GBR is a surgical method that attempts to regenerate damaged periodontal structures. It converts a tooth's prognosis from "questionable" to "favorable" in most cases, significantly impacting patients' quality of life. In these approaches, a barrier membrane is used to prevent soft tissue migration towards the defect, while also maintaining the wound space to provide a sheltered niche for host progenitor cells from the residual PDL, adjacent alveolar bone, or blood to recolonize the periodontal defect area and differentiate it into new supporting apparatus. Traditionally, GTR/GBR membranes are either non-resorbable or resorbable materials (Bottino et al., 2012). The most often used non-resorbable membranes are polytetrafluoroethylene (PTFE) membranes in the form of either high-density or titanium-reinforced high-density PTFE (Cucchi & Ghensi, 2014). Non-resorbable materials are biocompatible and have been shown in clinical studies to be effective; however, they are biologically inert and, instead, simply serve as a physical barrier (Bottino et al., 2012).

Furthermore, their use necessitates a second surgery to remove them, further increasing patient distress and the risk of infection at the surgical site (Aytac et al., 2021). As a result, a range of resorbable materials has been developed to substitute for non-resorbable materials. Natural, synthetic, or composite materials can be utilized to engineer resorbable membranes with tunable degradation properties (Reise et al., 2012). However, existing resorbable membranes have well-known and inherent flaws, such as poor adhesion to surrounding tissues, a lack of restorative qualities, and limited regeneration potential (Bottino et al., 2012).

Bone regeneration is concomitant to the neoformation of cementum and PDL in the periodontium's intricate multi-tissue complexity and architecture. Recent advances in tissue engineering and the evolving field of biofabrication have remarkably enhanced regenerative medicine's clinical outcomes. Additionally, they have also raised innovative prospects for the predictable translation of personalized and more foreseeable bone and periodontal regeneration strategies (Daghrery et al., 2022). The advancement in technique and materials has fostered the manufacture of multifunctional membranes. Such membranes possess tunable mechanical and biophysical properties, propelling the field toward biomimetic multi-tissue regeneration.

To date, a therapeutically translatable scaffold for craniofacial bone and periodontal tissue regeneration can be processed via 3D printing technologies (Aytac et al., 2021). 3D printing, an additive manufacturing



method, has been lauded as a paradigm shift empowering regenerative dental medicine. 3D printing allows layer-by-layer deposition of polymeric materials to generate a 3D anatomically complex construct. To simultaneously guide the coordinated regeneration of periodontal tissue complex, 3D printing strategies currently entail creating monophasic or multiphasic scaffolds with macroscale, microscale, and nanoscale features. These features are tunable via controlling scaffold structure, pore size for bone zone, fiber alignment for PDL zone, and surface topography (Daghrery et al., 2022). For example, triphasic scaffolds were formed using 3D printed PCL scaffolds and electrospun PLGA nanofibers, which closely imitate the zonal milieu of a bone-to-ligament interface by controlling fiber spacing and fibers' bone-ligament alignment. This scaffold reproduced the gradient structural bone-ligament components while improving ligamentogenesis (Criscenti et al., 2016).

Regarding scaffold macrostructural features, controlled porosity, e.g., up to 700  $\mu\text{m}$ , resulted in higher osteogenic differentiation of pre-osteoblasts *in vitro* and promoted substantial bone and blood vessel formation *in vivo* upon implantation into rabbit calvaria defects (Shim et al., 2017). Importantly, 3D printed polymeric scaffolds can be loaded with therapeutic agents (e.g., dexamethasone) to induce the osteogenic differentiation of host mesenchymal stem cells (Costa et al., 2015). Similarly, in the layer-by-layer deposition of PLA polymeric material, the scaffolds exhibited a well-ordered pore size of 200  $\mu\text{m}$ , promoting the release of angiogenic and osteogenic growth factors (GFs) to build vascularized bone structures (Cui et al., 2016). The synchronized release pattern of the GFs – the core of the scaffold loaded with bone morphogenetic protein 2 (BMP2) and its outside surface activated with connective tissue growth factor (CTGF), boosted vascularized bone regeneration *in vivo* (Cheng et al., 2019).

Melt electrowriting (MEW) is an alternative to traditional thermal extrusion of melted polymer and solution electrospinning methods. MEW consolidates thermal polymer extrusion and electrospinning technique principles to print micron- to nano-sized filaments, which are often 10 orders of magnitude thinner than conventional printed scaffolds (Daghrery et al., 2022). Processing flexibility, control of scaffold shape, porosity, and fiber diameter are significantly important for bone and periodontal tissue engineering. Remarkably, control over layer deposition for the fabrication of graded MEW scaffolds and post-processing modification with osteoconductive coating, e.g., CaP, resulted in superior bone healing potential in calvaria

defects (**Figure 3A**) (Abbasi et al., 2020). The porous scaffold and porosity gradient produce a 3D design that closely resembles natural bone architecture by steadily increasing the size of pores in each printed layer, simulating the mineral density variations from cortical toward cancellous bone (**Figure 3A1-A2**) (Abbasi et al., 2020). Analogously, melt electrowritten poly(lactide-block-ethylene glycol-block-lactide) (PLA-PEG-PLA) scaffolds comprising 45S5 BG have also been demonstrated to exhibit bioactive properties for bone tissue engineering applications (Hochleitner et al., 2017).

Recently, our group reported on the manufacture of highly-ordered MEW polymeric (PCL) scaffolds coated with a unique nanostructured fluorinated calcium phosphate (F/CaP) layer (**Figure 3B**) (Daghrery et al., 2021). The innovative nanostructured F/CaP coating led to a superior osteogenic differentiation of periodontal ligament stem cells (PDLSCs), while attenuating the growth of *P. gingivalis*, a common bacterium in periodontics. Moreover, *in vivo* findings confirm the periodontal regenerative capacity when implanted in a fenestration defect model (**Figure 3B1**). Briefly, F/CaP nanostructured scaffolds acted not only as a barrier to prevent soft tissue ingrowth but also supported host progenitor cells to regenerate the periodontium (Daghrery et al., 2021). Hence, highly ordered 3D printed scaffolds provide a new avenue for elaborating personalized scaffolds that promote tissue-specific differentiation of progenitor cells and, as a result, guide the simultaneous and coordinated regeneration of periodontal tissues and tissue interfaces (**Figure 3B2-B3**).

Hydrogel-based bioprinting develops cell-laden constructs with well-defined and geometrically competent functional tissue constructs (Aytac et al., 2021). In our group's recent work, a bioprinted hydrogel containing amorphous magnesium phosphate (AMP) bioactive particles has demonstrated a significant increase in osteogenesis (Dubey et al., 2020) (**Figure 4A**). The cell-free AMP-loaded construct shows superior bone healing potential after implantation in calvarial defects. Notably, the bioactive potential of AMPs was sufficient to induce osteogenic differentiation of endogenous cells, providing an alternative to generally used osteoinductive GFs, e.g., BMP2.

In periodontics, the prime goal is to develop bioactive multifunctional constructs that operate as a physical barrier to inhibit soft tissue ingrowth. These constructs must have suitable mechanical and physical properties to sufficiently withstand prolonged stresses and execute barrier roles. Although hydrogels have been employed to aid cell differentiation, they are soft by nature and lack the mechanical strength required for load-

bearing applications (Daghery et al., 2022). As a result, hydrogel reinforcement with polymeric 3D printed (MEW) meshes, such as reinforced constructs of MEW/PCL integrated into gelatin methacryloyl (GelMA) hydrogels, offers the possibility of mimicking the biological and mechanical microenvironments of human tissue (Dubey et al., 2020) (**Figure 4B**). Such integration resulted in a mechanical competency, while the presence of AMP provided a therapeutic feature (**Figure 4B1**) (Dubey et al., 2020). The engineered multifunctional membrane displayed tunable properties that prevented soft tissue invasion and maximized bone formation *in vivo* (Dubey et al., 2020) (**Figure 4B2-B3**). Undoubtedly, 3D (bio)printing offers tremendous translational potential for craniofacial and periodontal tissue regeneration (Aytac et al., 2021). In particular, periodontal-related cell types can be feasibly bioprinted and tailored for personalized therapeutics to guide the coordinated regeneration of soft and mineralized periodontal tissues. Moreover, the convergence of distinct tissue engineering approaches into a single platform holds promise for reconstructing highly-ordered tissues and tissue interfaces (Daghery et al., 2022).

### 3.3 Cues for Cementum Formation

Cementum, also known as root cementum, is an avascular mineralized tissue lining the surface of the root (Yamamoto et al., 2016). Scaffolds that solely capture bone and PDL compartments, for example, failed to generate cementum on a periodontal defect's root surface (Dan et al., 2014; Yu et al., 2022). Hence, multiphasic/biphasic scaffolds with a structural arrangement, as well as distinct architectural and bioactive cues, should be designed to emulate the periodontium's zonal structure to facilitate multi-tissue regeneration (Liang et al., 2020; Daghery et al., 2022). Because each zone of the periodontium has individual features, each tissue-specific zone of the intended scaffold should be built correspondingly to create a multi-tissue design. The hierarchical zonal-specific regenerative cues, *e.g.*, amelogenin (cement), connective tissue growth factor (PDL), and BMP-2 (bone), can boost tissue-specific cell differentiation (Lee et al., 2014). However, a proper carrier system should be considered to sustain biological availability (Aytac et al., 2021). For instance, polyethylene glycol (PEG)-stabilized amorphous calcium phosphate (ACP) nanoparticles loaded with recombinant human cementum protein 1 (rhCEMP1) had been electrospun into multiphasic scaffolds, including PCL, type I collagen, and rhCEMP1/ACP. When tested in an appropriate *in vivo* periodontal defect, the controlled release promoted cementum-like tissue formation with a limited amount of bone fill after 8

weeks (Chen et al., 2016). Moreover, to restore the periodontium, a composite scaffold of chitin-PLGA-nanobioactive glass was manufactured (Sowmya et al., 2017). The use of nanobioactive glass in combination with growth factors, including platelet-rich plasma-derived growth factors, fibroblast growth factor 2, and cementum protein 1 enclosed within a porous tri-layered nanocomposite hydrogel scaffold, led to periodontal tissue regeneration in rabbit maxillary defects (Sowmya et al., 2017).

Nonetheless, cementogenesis, the neoformation of cementum, is difficult since it is heavily dependent on endogenous progenitor cells to support cement deposition. Therefore, Vaquette et al. (2012) used PCL and 20% TCP to produce biphasic 3D printed scaffolds with approximately 70% internal porosity and full interconnectivity to build the bone zone. Meanwhile, the PDL zone was generated by electrospinning PCL solution to support and distribute mature PDL cell sheets (Vaquette et al., 2012). The biphasic scaffold-supported cell sheets were attached to a dentin slice and implanted subcutaneously in athymic rats. It has been reported that 67% of the PDL cell sheet test group had new cementum-like tissue on the dentin surface, compared to only 17% of the non-cell sheet group. The highly specialized design of biphasic/multiphasic scaffolds for bone and PDL zones enhances outcomes and paves the way for new tissue-specific regenerative approaches.

The composition and architecture of zonal, tissue-specific scaffolds have been considered critical for coordinating the growth and guiding the regeneration of both soft and mineralized periodontal tissues. Remarkably, a biphasic scaffold of solution electrospinning and melt electrowriting has established a delivery system for matured cell sheets made up of periodontal ligament cells (PDLC), gingival cells, and bone marrow-derived MSCs. In a sheep periodontal defect model, MEW was used to generate the bone zone, and the presence of a macroscopic porosity of  $220 \pm 141 \mu\text{m}$  facilitated tissue ingrowth, while a flexible electrospun scaffold enabled cell sheet transport. The *in vivo* findings showed tissue integration between bone and PDL (Vaquette et al., 2019).

### **3.4 Cues for PDL Formation**

The periodontal complex secures the tooth to the jawbone and provides a protective barrier for the underlying structures. PDL collagen fibers' unmineralized network provides flexible attachment between alveolar bone and cementum. It is widely established that periodontium is a multi-structural, functional unit,

and that restoring either one or two elements of the periodontium is inadequate for restoring physiological periodontal functions (Daghrery et al., 2022). While different cells from various sources could be used to construct cell sheets, bone marrow mesenchymal stem cell sheets and PDL cell sheets outperformed gingival cells in terms of new bone, PDL, and cementum regeneration (Vaquette et al., 2019). It has been reported that the multilayer scaffold of bone, PDL compartments, and cell sheets resulted in PDL- and cementum-like tissue formation when adapted to the dentin slice model (Vaquette et al., 2012). Even though the PDL fiber-like structure was formed using multilayer cell sheets, the inserted fibers were randomly scattered. Remarkably, the aligned PDL fibers provide a functional link between the cementum and alveolar bone. Failure to resemble those structures obstructs the formation of a competent periodontal complex. As a result, the classic approach to approximating PDL's extracellular matrix (ECM) architecture closely mimics fiber alignment. Several strategies for inducing PDL fiber alignment have been developed, such as microchanneling, micropatterned constructs, and electrospinning of aligned nanofibrous matrices (Park et al., 2014; Pilipchuk et al., 2018; Ren et al., 2017).

Orientations of the PDL primary fibers define the structure of the newly formed PDL tissue. The polymeric platform's multi-channel architecture affects cell orientation on the matrix's surfaces. For instance, a computer-aided (CAD-based) design of a microchannel fiber-guiding mold allows the molten polymer to shape micropatterned scaffolds with various pillars to induce fiber's alignment (Pilipchuk et al., 2018). Moreover, scaffold immobilization with platelet-derived growth factor-BB (AdPDGF-BB) and bone morphogenetic protein-7 (AdBMP-7) enables spatial gene delivery, alongside micropatterning-guided ligamentous tissue formation and improved periodontal bone-PDL regeneration in large osseous defects (**Figure 5A**) (Pilipchuk et al., 2018). In one study, microgrooves were employed to guide cell orientations in parallel (0°), oblique (45°), and perpendicular (90°) angulations (**Figure 5B**) (Park et al., 2017). Apart from the structural simulation of the PDL using this approach, regeneration of functional PDL is also a factor to consider, necessitating different functional and mechanical analyses. However, these scaffolds barely guided periodontal regeneration; the failure likely occurred because the guiding platform is higher in magnitude than native structures.

Additive manufacturing (AM) methods, including fused deposition modeling (FDM) and selective laser sintering (SLS), have been utilized in a patient-specific and personalized scaffold for periodontal tissue regeneration. However, the FDM- or SLS-printed constructs are generally bulky, interfering with tissue ingrowth and stability (Rasperini et al., 2015; Schumann et al., 2007). Therefore, in recent years, nanofibrous and multiphasic biomimetic scaffolds have been designed for periodontal tissue regeneration to create an ECM-like microenvironment. The nanofibrous scaffolds create an ECM-like environment that aids fibroblast development and PDL-specific marker expression (Ren et al., 2017; Daghery et al., 2023). Electrospinning is a straightforward method for manufacturing oriented and highly aligned nanofibrous fiber mats (Daghery et al., 2020). The aligned electrospun fibers guide cell elongation and collagen fibers' orientation on the scaffold surface. For instance, a 3D multilayered scaffold of highly aligned biodegradable PCL/polyethylene glycol copolymer nanofibrous mats impregnated into porous chitosan (CHI) offered topographic cues to guide periodontal tissue regeneration (**Figure 5C**) (Jiang et al., 2015). The aligned nanofibers showed a more organized regenerated PDL pattern than their random counterpart, with a higher expression periostin level. However, electrospun scaffolds' densely-packed fibrous structure often limits cellular infiltration; it fails to generate scaffolds with patient-specific geometries (Daghery et al., 2021). Although various technologies show promise in regenerating craniofacial deformities, they fall short of facilitating the coordinated regeneration of soft and hard periodontal tissues, considering patient-specific geometries.

Alternatively, MEW/3D printing provides superior controlled fiber deposition, creating geometrically defined scaffolds for periodontal tissue regeneration (Daghery et al., 2021). Combining image-based processing and MEW/3D printing enables high-fidelity manufacture of personalized scaffolds for anatomically complicated structures (Daghery et al., 2022). A recent effort by our group to engineer personalized zonal-specific scaffolds was tailored to guide tissue-specific stem cell differentiation and direct macrophage polarization (**Figure 6**). The MEW technique was used to obtain scaffolds with control over fiber morphology and architectures, *e.g.*, aligned, random, and highly ordered 250  $\mu\text{m}$  and 500  $\mu\text{m}$  spacing. While fiber alignment promoted macrophage polarization toward the pro-healing M2 type and upregulated the expression of periostin, a ligamentogenic marker, the spacing of the fibers plays a vital role in Runx2 (an osteogenic marker) upregulation. Furthermore, *in vivo* investigations in a well-established periodontal fenestration defect

model strongly support the coordinated periodontal tissue regeneration of both hard (alveolar bone and cementum) and soft tissue (PDL) along the tooth root. Importantly, these findings suggest that MEW can be used to fabricate clinical scale and personalized scaffolds tailored with a high printing accuracy for regenerative periodontics (Daghrery et al., 2022).

#### **4. CONCLUSIONS**

Several hindrances stand in the way of decisive periodontal tissue regeneration. One critical concern is a shortage of comprehensive fundamental biological and developmental knowledge. A systematic understanding of basic biology is required to offer rigorous information to manufacture biomimetic materials and scaffolds. To accomplish successful periodontal tissue regeneration, it is necessary to accurately imitate the architecture of periodontal tissues at different scale levels. Biophysical and bioactive cues must be delivered spatially and temporally to manage the hierarchical architecture of the periodontium. The spatial regulation for cell migration, proliferation, and differentiation must be tailored to induce alveolar bone, PDL, and cementum regeneration simultaneously. The physiological, functional, and mechanical factors that have been shown to play a role in periodontal tissue regeneration should also be considered.

From a clinical standpoint, the periodontium consists of protective and supporting structures, and its interaction is critical for long-term oral health. Functional PDL fiber regeneration between cementum and alveolar bone is one of the main challenges in periodontal regeneration. Without these fibers, cementum-PDL-alveolar bone attachments are neither securely stable nor do they support teeth against occlusal load. As a result, innovative and bioinspired constructs that closely mirror periodontal tissues' architecture are needed to engineer personalized and defect-specific scaffolds to more predictably promote the regeneration of the periodontium.

**Funding information:** National Institute of Dental and Craniofacial Research, Grant/Award Numbers: R01DE031476 and R01DE026578 to M.C.B.; National Institutes of Health.

#### **AUTHOR CONTRIBUTIONS**

Arwa Daghery: contributed to conception, design, and drafted the manuscript. Marco C. Bottino: contributed to conception, design, drafted the manuscript, and critically revised the manuscript.

All authors gave the final approval and agreed to be accountable for all aspects of the work.

#### **ACKNOWLEDGMENTS**

M.C.B. acknowledges the National Institutes of Health/NIH (National Institute of Dental and Craniofacial Research, grants R01DE026578 and R01DE031476), the OsteoScience Foundation (Peter Geistlich Research Award), and the American Academy of Implant Dentistry Foundation (AAIDF). The content is solely the responsibility of the authors and does not necessarily represent the official views of the National Institutes of Health.

#### **CONFLICT OF INTEREST**

The authors declare no conflict of interest.

#### **DATA AVAILABILITY STATEMENT**

Data sharing is not applicable to this article as no new data were created or analyzed in this study.



## REFERENCES

- Abbasi, N., Ivanovski, S., Gulati, K., Love, R. M., & Hamlet, S. (2020). Role of offset and gradient architectures of 3-D melt electrowritten scaffold on differentiation and mineralization of osteoblasts. *Biomaterials Research*, *24*(1), 2. <https://doi.org/10.1186/s40824-019-0180-z>
- Abbasi, N., Lee, R. S. B., Ivanovski, S., Love, R. M., & Hamlet, S. (2020). In vivo bone regeneration assessment of offset and gradient melt electrowritten (MEW) PCL scaffolds. *Biomaterials Research*, *24*(1), 17. <https://doi.org/10.1186/s40824-020-00196-1>
- Aytac, Z., Dubey, N., Dagherery, A., Ferreira, J. A., Araújo, I. J. de S., Castilho, M., Malda, J., & Bottino, M. C. (2021). Innovations in craniofacial bone and periodontal tissue engineering – from electrospinning to converged biofabrication. *International Materials Reviews*, *0*(0), 1–38. <https://doi.org/10.1080/09506608.2021.1946236>
- Bottino, M. C., Thomas, V., Schmidt, G., Vohra, Y. K., Chu, T.-M. G., Kowolik, M. J., & Janowski, G. M. (2012). Recent advances in the development of GTR/GBR membranes for periodontal regeneration—A materials perspective. *Dental Materials*, *28*(7), 703–721. <https://doi.org/10.1016/j.dental.2012.04.022>
- Chen, X., Liu, Y., Miao, L., Wang, Y., Ren, S., Yang, X., Hu, Y., & Sun, W. (2016). Controlled release of recombinant human cementum protein 1 from electrospun multiphasic scaffold for cementum regeneration. *International Journal of Nanomedicine*, *11*, 3145–3158. <https://doi.org/10.2147/IJN.S104324>
- Cheng, G., Yin, C., Tu, H., Jiang, S., Wang, Q., Zhou, X., Xing, X., Xie, C., Shi, X., Du, Y., Deng, H., & Li, Z. (2019). Controlled Co-delivery of Growth Factors through Layer-by-Layer Assembly of Core-Shell Nanofibers for Improving Bone Regeneration. *ACS Nano*, *13*(6), 6372–6382. <https://doi.org/10.1021/acsnano.8b06032>
- Cho, M.-I., & Garant, P. R. (2000). Development and general structure of the periodontium. *Periodontology* *2000*, *24*(1), 9–27. <https://doi.org/10.1034/j.1600-0757.2000.2240102.x>

- Costa, P. F., Puga, A. M., Díaz-Gomez, L., Concheiro, A., Busch, D. H., & Alvarez-Lorenzo, C. (2015). Additive manufacturing of scaffolds with dexamethasone controlled release for enhanced bone regeneration. *International Journal of Pharmaceutics*, 496(2), 541–550. <https://doi.org/10.1016/j.ijpharm.2015.10.055>
- Criscenti, G., Longoni, A., Di Luca, A., De Maria, C., van Blitterswijk, C. A., Vozzi, G., & Moroni, L. (2016). Triphasic scaffolds for the regeneration of the bone-ligament interface. *Biofabrication*, 8(1), 015009. <https://doi.org/10.1088/1758-5090/8/1/015009>
- Cucchi, A., & Ghensi, P. (2014). Vertical Guided Bone Regeneration using Titanium-reinforced d-PTFE Membrane and Prehydrated Corticocancellous Bone Graft. *The Open Dentistry Journal*, 8, 194–200. <https://doi.org/10.2174/1874210601408010194>
- Cui, H., Zhu, W., Holmes, B., & Zhang, L. G. (2016). Biologically Inspired Smart Release System Based on 3D Bioprinted Perfused Scaffold for Vascularized Tissue Regeneration. *Advanced Science (Weinheim, Baden-Wuerttemberg, Germany)*, 3(8), 1600058. <https://doi.org/10.1002/advs.201600058>
- Daghery, A., Aytac, Z., Dubey, N., Mei, L., Schwendeman, A., & Bottino, M. C. (2020). Electrospinning of dexamethasone/cyclodextrin inclusion complex polymer fibers for dental pulp therapy. *Colloids and Surfaces B: Biointerfaces*, 111011. <https://doi.org/10.1016/j.colsurfb.2020.111011>
- Daghery, A., de Souza Araújo, I. J., Castilho, M., Malda, J., & Bottino, M. C. (2022). Unveiling the potential of melt electrowriting in regenerative dental medicine. *Acta Biomaterialia*. <https://doi.org/10.1016/j.actbio.2022.01.010>
- Daghery, A., Ferreira, J. A., de Souza Araújo, I. J., Clarkson, B. H., Eckert, G. J., Bhaduri, S. B., Malda, J., & Bottino, M. C. (2021). A Highly Ordered, Nanostructured Fluorinated CaP-Coated Melt Electrowritten Scaffold for Periodontal Tissue Regeneration. *Advanced Healthcare Materials*, e2101152. <https://doi.org/10.1002/adhm.202101152>
- Dan, H., Vaquette, C., Fisher, A. G., Hamlet, S. M., Xiao, Y., Hutmacher, D. W., & Ivanovski, S. (2014). The influence of cellular source on periodontal regeneration using calcium phosphate coated polycaprolactone scaffold supported cell sheets. *Biomaterials*, 35(1), 113–122. <https://doi.org/10.1016/j.biomaterials.2013.09.074>
- Dangaria, S. J., Ito, Y., Luan, X., & Diekwisch, T. G. H. (2011). Successful Periodontal Ligament Regeneration by Periodontal Progenitor Preseeding on Natural Tooth Root Surfaces. *Stem Cells and Development*, 20(10), 1659–1668. <https://doi.org/10.1089/scd.2010.0431>
- Dubey, N., Ferreira, J. A., Daghery, A., Aytac, Z., Malda, J., Bhaduri, S. B., & Bottino, M. C. (2020). Highly tunable bioactive fiber-reinforced hydrogel for guided bone regeneration. *Acta Biomaterialia*. <https://doi.org/10.1016/j.actbio.2020.06.011>
- Dubey, N., Ferreira, J. A., Malda, J., Bhaduri, S. B., & Bottino, M. C. (2020). Extracellular Matrix/Amorphous Magnesium Phosphate Bioink for 3D Bioprinting of Craniomaxillofacial Bone Tissue. *ACS Applied Materials & Interfaces*, 12(21), 23752–23763. <https://doi.org/10.1021/acsami.0c05311>
- Eke, P. I., Dye, B. A., Wei, L., Slade, G. D., Thornton-Evans, G. O., Borgnakke, W. S., Taylor, G. W., Page, R. C., Beck, J. D., & Genco, R. J. (2015). Update on Prevalence of Periodontitis in Adults in the United States: NHANES 2009 – 2012. *Journal of Periodontology*, 86(5), 611–622. <https://doi.org/10.1902/jop.2015.140520>
- Ferreira, J. A., Kantorski, K. Z., Dubey, N., Daghery, A., Fenno, J. C., Mishina, Y., Chan, H.-L., Mendonça, G., & Bottino, M. C. (2021). Personalized and Defect-Specific Antibiotic-Laden Scaffolds for Periodontal Infection Ablation. *ACS Applied Materials & Interfaces*, 13(42), 49642–49657. <https://doi.org/10.1021/acsami.1c11787>
- Friesen, L. R., Williams, K. B., Krause, L. S., & Killoy, W. J. (2002). Controlled local delivery of tetracycline with polymer strips in the treatment of periodontitis. *Journal of Periodontology*, 73(1), 13–19. <https://doi.org/10.1902/jop.2002.73.1.13>
- Furtos, G., Rivero, G., Rapuntean, S., & Abraham, G. A. (2017). Amoxicillin-loaded electrospun nanocomposite membranes for dental applications. *Journal of Biomedical Materials Research Part B: Applied Biomaterials*, 105(5), 966–976. <https://doi.org/10.1002/jbm.b.33629>
- Hu, Z., Ma, C., Rong, X., Zou, S., & Liu, X. (2018). Immunomodulatory ECM-like Microspheres for Accelerated Bone Regeneration in Diabetes Mellitus. *ACS Applied Materials & Interfaces*, 10(3), 2377–2390. <https://doi.org/10.1021/acsami.7b18458>

- Jiang, W., Li, L., Zhang, D., Huang, S., Jing, Z., Wu, Y., Zhao, Z., Zhao, L., & Zhou, S. (2015). Incorporation of aligned PCL-PEG nanofibers into porous chitosan scaffolds improved the orientation of collagen fibers in regenerated periodontium. *Acta Biomaterialia*, 25, 240–252. <https://doi.org/10.1016/j.actbio.2015.07.023>
- Könönen, E., Gursoy, M., & Gursoy, U. K. (2019). Periodontitis: A Multifaceted Disease of Tooth-Supporting Tissues. *Journal of Clinical Medicine*, 8(8), 1135. <https://doi.org/10.3390/jcm8081135>
- Lee, C. H., Hajibandeh, J., Suzuki, T., Fan, A., Shang, P., & Mao, J. J. (2014). Three-Dimensional Printed Multiphase Scaffolds for Regeneration of Periodontium Complex. *Tissue Engineering. Part A*, 20(7–8), 1342–1351. <https://doi.org/10.1089/ten.tea.2013.0386>
- Lee, S.-B., Lee, D.-Y., Lee, Y.-K., Kim, K.-N., Choi, S.-H., & Kim, K.-M. (2008). Surface modification of a guided tissue regeneration membrane using tetracycline-containing biodegradable polymers. *Surface and Interface Analysis*, 40(3-4), 192–197. <https://doi.org/10.1002/sia.2761>
- Liang, Y., Luan, X., & Liu, X. (2020). Recent advances in periodontal regeneration: A biomaterial perspective. *Bioactive Materials*, 5(2), 297–308. <https://doi.org/10.1016/j.bioactmat.2020.02.012>
- Lin, H.-Y., Chang, T.-W., & Peng, T.-K. (2018). Three-dimensional plotted alginate fibers embedded with diclofenac and bone cells coated with chitosan for bone regeneration during inflammation. *Journal of Biomedical Materials Research. Part A*, 106(6), 1511–1521. <https://doi.org/10.1002/jbm.a.36357>
- M, H., H, J., R, W., Y, X., & C, Z. (2017). Fabrication of metronidazole loaded poly ( $\epsilon$ -caprolactone)/zein core/shell nanofiber membranes via coaxial electrospinning for guided tissue regeneration. *Journal of Colloid and Interface Science*, 490. <https://doi.org/10.1016/j.jcis.2016.11.062>
- Nasajpour, A., Ansari, S., Rinoldi, C., Rad, A. S., Aghaloo, T., Shin, S. R., Mishra, Y. K., Adelung, R., Swieszkowski, W., Annabi, N., Khademhosseini, A., Moshaverinia, A., & Tamayol, A. (2018). A Multifunctional Polymeric Periodontal Membrane with Osteogenic and Antibacterial Characteristics. *Advanced Functional Materials*, 28(3), 1703437. <https://doi.org/10.1002/adfm.201703437>
- Ngawhirunpat, T., Opanasopit, P., Rojanarata, T., Akkaramongkolporn, P., Ruktanonchai, U., & Supaphol, P. (2009). Development of meloxicam-loaded electrospun polyvinyl alcohol mats as a transdermal therapeutic agent. *Pharmaceutical Development and Technology*, 14(1), 70–79. <https://doi.org/10.1080/10837450802409420>
- Palma, P. J., Ramos, J. C., Martins, J. B., Diogenes, A., Figueiredo, M. H., Ferreira, P., Viegas, C., & Santos, J. M. (2017). Histologic Evaluation of Regenerative Endodontic Procedures with the Use of Chitosan Scaffolds in Immature Dog Teeth with Apical Periodontitis. *Journal of Endodontics*, 43(8), 1279–1287. <https://doi.org/10.1016/j.joen.2017.03.005>
- Park, C. H., Kim, K. H., Rios, H. F., Lee, Y. M., Giannobile, W. V., & Seol, Y. J. (2014). Spatiotemporally Controlled Microchannels of Periodontal Mimic Scaffolds. *Journal of Dental Research*, 93(12), 1304–1312. <https://doi.org/10.1177/0022034514550716>
- Park, C. H., Kim, K.-H., Lee, Y.-M., Giannobile, W. V., & Seol, Y.-J. (2017). 3D Printed, Microgroove Pattern-Driven Generation of Oriented Ligamentous Architectures. *International Journal of Molecular Sciences*, 18(9). <https://doi.org/10.3390/ijms18091927>
- Pilipchuk, S. P., Fretwurst, T., Yu, N., Larsson, L., Kavanagh, N. M., Asa'ad, F., Cheng, K. C. K., Lahann, J., & Giannobile, W. V. (2018). Micropatterned Scaffolds with Immobilized Growth Factor Genes Regenerate Bone and Periodontal Ligament-Like Tissues. *Advanced Healthcare Materials*, 7(22), e1800750. <https://doi.org/10.1002/adhm.201800750>
- Rasperini, G., Pilipchuk, S. P., Flanagan, C. L., Park, C. H., Pagni, G., Hollister, S. J., & Giannobile, W. V. (2015). 3D-printed Bioresorbable Scaffold for Periodontal Repair. *Journal of Dental Research*. <https://doi.org/10.1177/0022034515588303>
- Reise, M., Wyrwa, R., Müller, U., Zylinski, M., Völpel, A., Schnabelrauch, M., Berg, A., Jandt, K. D., Watts, D. C., & Sigusch, B. W. (2012). Release of metronidazole from electrospun poly(L-lactide-co-D/L-lactide) fibers for local periodontitis treatment. *Dental Materials: Official Publication of the Academy of Dental Materials*, 28(2), 179–188. <https://doi.org/10.1016/j.dental.2011.12.006>
- Ren, S., Yao, Y., Zhang, H., Fan, R., Yu, Y., Yang, J., Zhang, R., Liu, C., Sun, W., & Miao, L. (2017). Aligned Fibers Fabricated by Near-Field Electrospinning Influence the Orientation and Differentiation of hPDLSCs for Periodontal Regeneration. *Journal of Biomedical Nanotechnology*, 13(12), 1725–1734. <https://doi.org/10.1166/jbn.2017.2451>

- Ribeiro, J. S., Bordini, E. A. F., Ferreira, J. A., Mei, L., Dubey, N., Fenno, J. C., Piva, E., Lund, R. G., Schwendeman, A., & Bottino, M. C. (2020). Injectable MMP-Responsive Nanotube-Modified Gelatin Hydrogel for Dental Infection Ablation. *ACS Applied Materials & Interfaces*, *12*(14), 16006–16017. <https://doi.org/10.1021/acsami.9b22964>
- Ribeiro, J. S., Dagherery, A., Dubey, N., Li, C., Mei, L., Fenno, J. C., Schwendeman, A., Aytac, Z., & Bottino, M. C. (2020). Hybrid Antimicrobial Hydrogel as Injectable Therapeutics for Oral Infection Ablation. *Biomacromolecules*, *21*(9), 3945–3956. <https://doi.org/10.1021/acs.biomac.0c01131>
- Schumann, D., Ekaputra, A. K., Lam, C. X. F., & Hutmacher, D. W. (2007). Biomaterials/scaffolds. Design of bioactive, multiphasic PCL/collagen type I and type II-PCL-TCP/collagen composite scaffolds for functional tissue engineering of osteochondral repair tissue by using electrospinning and FDM techniques. *Methods in Molecular Medicine*, *140*, 101–124.
- Shahi, R. G., Albuquerque, M. T. P., Münchow, E. A., Blanchard, S. B., Gregory, R. L., & Bottino, M. C. (2017). Novel bioactive tetracycline-containing electrospun polymer fibers as a potential antibacterial dental implant coating. *Odontology*, *105*(3), 354–363. <https://doi.org/10.1007/s10266-016-0268-z>
- Shim, J.-H., Won, J.-Y., Park, J.-H., Bae, J.-H., Ahn, G., Kim, C.-H., Lim, D.-H., Cho, D.-W., Yun, W.-S., Bae, E.-B., Jeong, C.-M., & Huh, J.-B. (2017). Effects of 3D-Printed Polycaprolactone/ $\beta$ -Tricalcium Phosphate Membranes on Guided Bone Regeneration. *International Journal of Molecular Sciences*, *18*(5), 899. <https://doi.org/10.3390/ijms18050899>
- Sowmya, S., Mony, U., Jayachandran, P., Reshma, S., Kumar, R. A., Arzate, H., Nair, S. V., & Jayakumar, R. (2017). Tri-Layered Nanocomposite Hydrogel Scaffold for the Concurrent Regeneration of Cementum, Periodontal Ligament, and Alveolar Bone. *Advanced Healthcare Materials*, *6*(7), 1601251. <https://doi.org/10.1002/adhm.201601251>
- Torabi, S., & Soni, A. (2021). Histology, Periodontium. In *StatPearls [Internet]*. StatPearls Publishing. <https://www.ncbi.nlm.nih.gov/books/NBK570604/>
- Vaquette, C., Fan, W., Xiao, Y., Hamlet, S., Hutmacher, D. W., & Ivanovski, S. (2012). A biphasic scaffold design combined with cell sheet technology for simultaneous regeneration of alveolar bone/periodontal ligament complex. *Biomaterials*, *33*(22), 5560–5573. <https://doi.org/10.1016/j.biomaterials.2012.04.038>
- Vaquette, C., Saifzadeh, S., Farag, A., Hutmacher, D. W., & Ivanovski, S. (2019). Periodontal Tissue Engineering with a Multiphasic Construct and Cell Sheets. *Journal of Dental Research*, *98*(6), 673–681. <https://doi.org/10.1177/0022034519837967>
- Wang, X., Thibodeau, B., Trope, M., Lin, L. M., & Huang, G. T.-J. (2010). Histologic characterization of regenerated tissues in canal space after the revitalization/revascularization procedure of immature dog teeth with apical periodontitis. *Journal of Endodontics*, *36*(1), 56–63. <https://doi.org/10.1016/j.joen.2009.09.039>
- Xiong, J., Gronthos, S., & Bartold, P. M. (2013). Role of the epithelial cell rests of Malassez in the development, maintenance and regeneration of periodontal ligament tissues. *Periodontology 2000*, *63*(1), 217–233. <https://doi.org/10.1111/prd.12023>
- Yamamoto, T., Hasegawa, T., Yamamoto, T., Hongo, H., & Amizuka, N. (2016). Histology of human cementum: Its structure, function, and development. *The Japanese Dental Science Review*, *52*(3), 63–74. <https://doi.org/10.1016/j.jdsr.2016.04.002>
- Yamauchi, N., Nagaoka, H., Yamauchi, S., Teixeira, F. B., Miguez, P., & Yamauchi, M. (2011). Immunohistological characterization of newly formed tissues after regenerative procedure in immature dog teeth. *Journal of Endodontics*, *37*(12), 1636–1641. <https://doi.org/10.1016/j.joen.2011.08.025>
- Yao, S., Pan, F., Prpic, V., & Wise, G. E. (2008). Differentiation of Stem Cells in the Dental Follicle. *Journal of Dental Research*, *87*(8), 767–771. <https://www.ncbi.nlm.nih.gov/pmc/articles/PMC2553250/>
- Yu, M., Luo, D., Qiao, J., Guo, J., He, D., Jin, S., Tang, L., Wang, Y., Shi, X., Mao, J., Cui, S., Fu, Y., Li, Z., Liu, D., Zhang, T., Zhang, C., Li, Z., Zhou, Y., & Liu, Y. (2022). A hierarchical bilayer architecture for complex tissue regeneration. *Bioactive Materials*, *10*, 93–106. <https://doi.org/10.1016/j.bioactmat.2021.08.024>
- Zang, S., Mu, R., Chen, F., Wei, X., Zhu, L., Han, B., Yu, H., Bi, B., Chen, B., Wang, Q., & Jin, L. (2019). Injectable chitosan/ $\beta$ -glycerophosphate hydrogels with sustained release of BMP-7 and ornidazole in periodontal wound healing of class III furcation defects. *Materials Science and Engineering: C*, *99*, 919–928. <https://doi.org/10.1016/j.msec.2019.02.024>

## LIST OF CAPTIONS

**Figure 1.** A longitudinal section shows tooth-supporting structures of the periodontium in health (left) and disease (right). The periodontal complex comprises alveolar bone, gingiva, periodontal ligament [PDL], and cementum, all of which are gradually destroyed due to periodontitis. Adopted from Aytac et al. 2021.

**FIGURE 2.** Antibacterial and anti-inflammatory-therapeutics for periodontitis. **(A)** *In vivo* model to address infection ablation and tissue regeneration of the experimental periodontitis induced by ligature placement and *Pg* and *Fn* infection treated with antibiotic-laden scaffolds (1:3 MET/TCH) and Bio-Oss (BO). **(A<sub>1</sub>)** Three-dimensional  $\mu$ CT images [vestibular view] after 2- and 6-weeks post-treatment. The antibiotic-laden scaffold combined with BO showed lower bone loss when compared to the auto-healing control at 6 weeks. **(A<sub>2</sub>)** When compared to the auto-healing control, the antibiotic-laden (1:3 MET/TCH) scaffold + BO demonstrated statistically higher scores for mild inflammation and lower values for severe inflammation. Auto-healing, BO, and antibiotic-free scaffold + BO all showed identical mean percentages of mild inflammation (5%), whereas antibiotic-laden scaffold + BO (1:3 MET/TCH) showed 61% mild inflammation. Adopted from Ferreira et al. 2021. **(B)** Osteoimmunomodulatory IL-4-loaded NHG-MS and NG-MS and their release profiles, macrophage phenotype, and bone formation in the defect area. The macrophage phenotype in diabetes mellitus (DM) and the DM + heparin-modified gelatin microsphere (NHG-MS) groups had significantly higher levels of iNOS (green, M1 marker). There were significantly fewer M1 macrophages in the normal control and IL4-loaded NHG-MS DM groups compared to the other two DM groups, as evidenced by lower expression of iNOS. The IL4-loaded NHG-MS DM group had completely regenerated bone fill at the defect area after 4-weeks. Adopted from Hu et al., 2018.

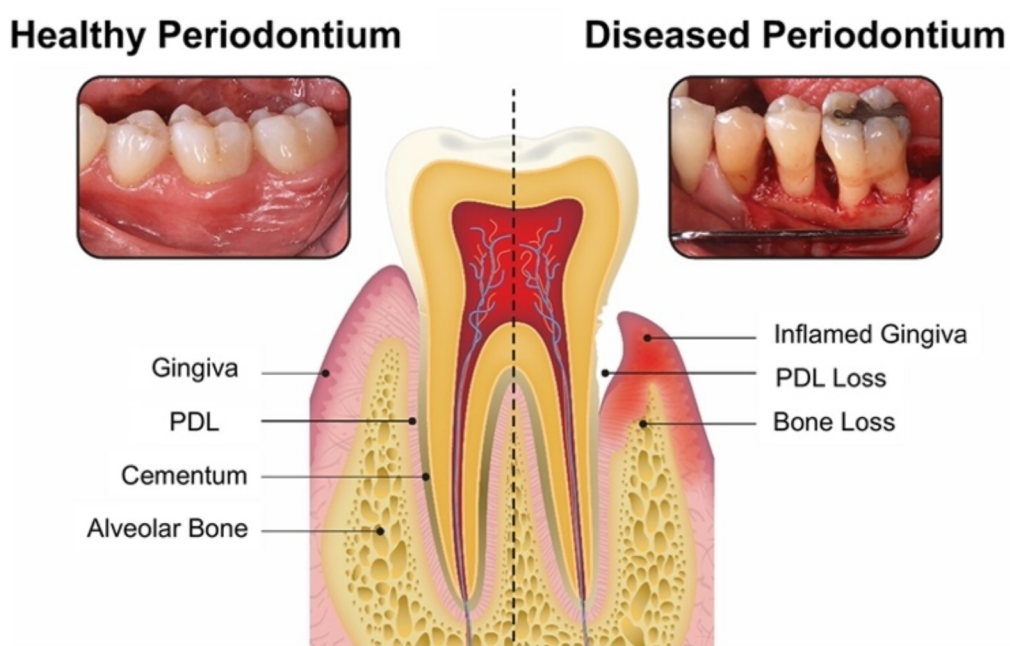
**FIGURE 3. (A)** Melt electrowritten polymeric (PCL) scaffolds for periodontal regeneration. **(A1)** Microscope images of H&E stained tissue sections of MEW PCL scaffolds implanted in rat calvarial defects. **(A2)** 3D reconstructed microCT image analysis shows the degree of bone repair in the different MEW PCL scaffolds implanted into the rat calvaria defect model. Defects treated with MEW scaffold that had 500  $\mu\text{m}$  pores and offset 50.50 structures showed new bone only at the defect periphery, while new bone formation increased toward the cavity center in the 250  $\mu\text{m}$  and both gradient (250top, 750top) scaffolds. At 8 weeks, the grad.250top showed significantly more new bone formation than the other groups. Adopted from Abbasi et al., 2020. **(B)** Highly ordered, nanostructured fluorinated CaP-coated MEW scaffold for periodontal tissue regeneration. Periodontal fenestration defect exposes the distal root of the first molar, 3- and 6-weeks post-implantation of F/CaP healing of the periodontium. At 3 weeks, F/CaP-coated scaffolds had significantly greater bone volume, bone fill, and tissue mineral density values than non-coated and sham groups. F/CaP-coated scaffolds at 6 weeks showed considerably more total bone coverage of the tooth roots. Adopted from Daghery et al., 2021.

**FIGURE 4.** 3D bioprinted scaffolds for alveolar bone regeneration. **(A)** 3D printed grid-like structures with sharp turns demonstrate the porous nature, showing elongated DPSCs' morphology in amorphous magnesium phosphate (AMP)-modified. In the calvaria defect, when the defects were filled with either ECM or ECM/1.0AMP, the bone repair was observed to be gradually. At 4 and 8 weeks, the BV/TV for ECM/1.0AMP was approximately 1.7- and 1.4-fold higher, respectively. The released  $\text{Mg}^{2+}$  ions stimulate osteoblast differentiation and increase mineralization. Adopted from Dubey et al., 2020. **(B)** Fiber-reinforced hydrogel with bioactive AMP gelatin methacryloyl hydrogels. The hydrogel fibers provide high stiffness and elasticity, and the presence of AMP enhances bone formation. The newly generated bone tissue in the GA5% group was almost 6-fold greater than the sham group, while the volume of new bone was increased by 8-fold in PCL mesh infused with GelMA + AMP hydrogel. Adopted Dubey et al., 2020.

**FIGURE 5.** Patterned polymeric scaffolds for periodontal tissue regeneration. **(A)** The PDL regions were either patterned or amorphous, while the bone regions were amorphous. The constructs are immobilized with adenoviral genes for Ad-BMP-7, Ad-PDGF-BB, or Ad-empty to promote ligamentous-like tissues and bone formation *in vivo*. The micropatterning regenerates soft tissue resembling the natural rat PDL's width of about 100  $\mu\text{m}$  and develops new bone in front of the patterned. Adopted from Pilipchuk et al., 2018. **(B)** Microgroove patterns created angulated ligament architectures. The cytoskeleton orientation of PDLSCs at 7- and 21-day cultures clearly follow the angulated patterns ( $\angle\text{Ligament} = 0^\circ, 45^\circ, \text{ and } 90^\circ$ ). Adopted from Park et al., 2017. **(C)** Periodontal fenestration defect at the maxillary first molar and implantation of layers of fibers placed perpendicular against the root. Picrosirius red staining for collagen formation in regenerated PDL-like tissue after 2 months. Type I collagen fibers (bright yellow-red/orange) and type III collagen fibers (green-blue) were visible in cross-polarized light pictures. In comparison to the other three groups (porous, 3D-Aligned, and 3D-Random), the fibers in the blank control group displayed a lower collagen type I/III ratio. While a considerably higher collagen I/III ratio was found in the aligned scaffold group, this indicates newly generated matured collagen fibers. Adopted from Jiang et al., 2015.

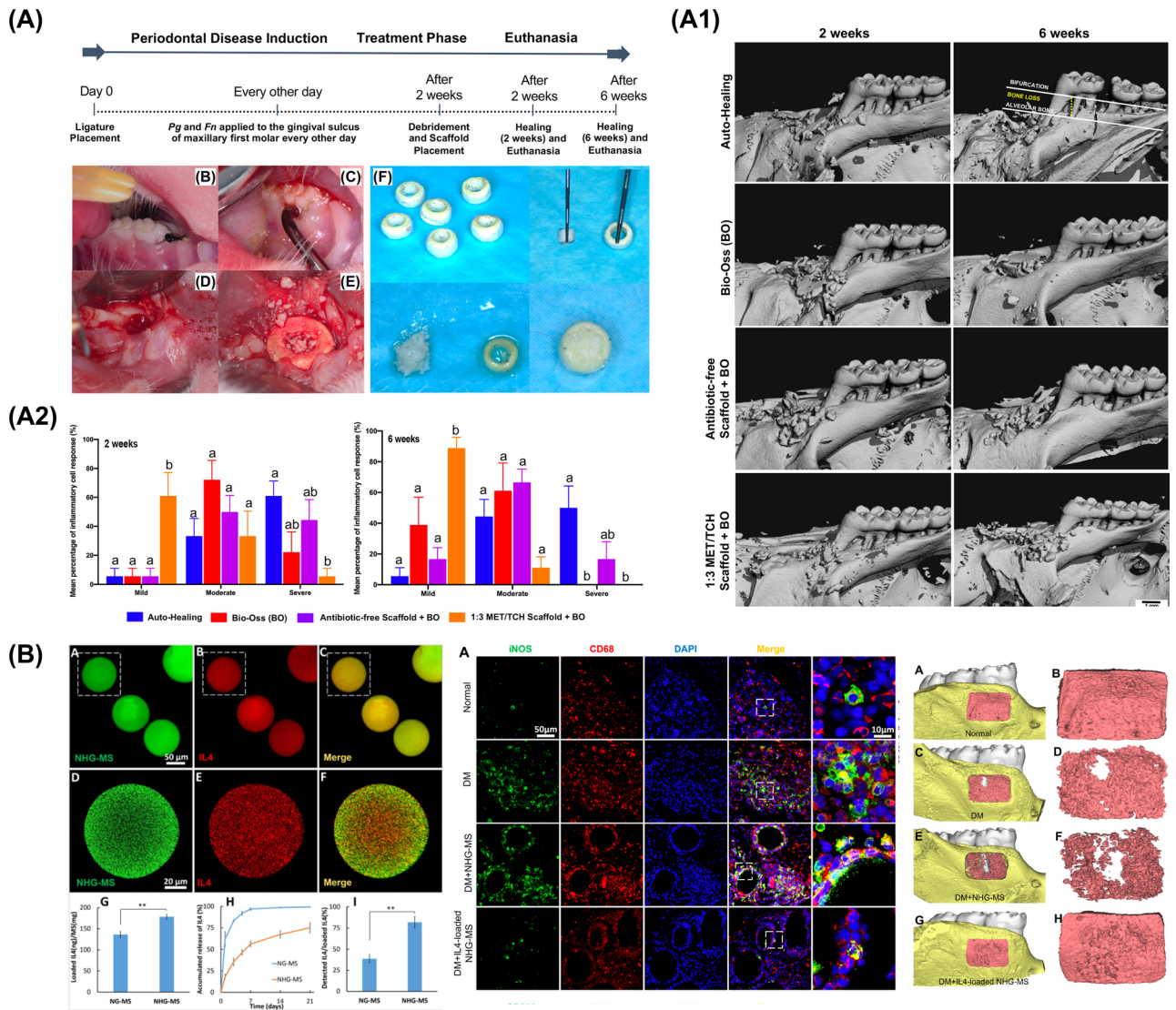
**Figure 6.** Image-based MEW engineered polymeric scaffold. **(A)** SEM images of MEW PCL scaffolds of different morphologies and architecture, e.g., aligned, random, and highly-ordered 250  $\mu\text{m}$  to 500  $\mu\text{m}$  spacing. **(B)** Changes in cell shape in response to scaffold design, directly affect PDLSCs commitment and macrophage polarization. Aligned MEW fibers direct hPDLSCs' orientation, promote ligamentogenesis, and drive macrophage polarization toward pro-healing M2. **(C)** Periodontal fenestration defect in rat mandible. **(D)** 3D reconstructed micro-CT images of the defect and image data were used to print a personalized periodontal scaffold. The scaffolds showed exterior macrostructure distinctive to defects and internal tissue-specific

microstructure. The personalized scaffolds exhibited a high printing accuracy of  $0.7 \pm 0.1$ . Adopted from Daghery et al. 2022.

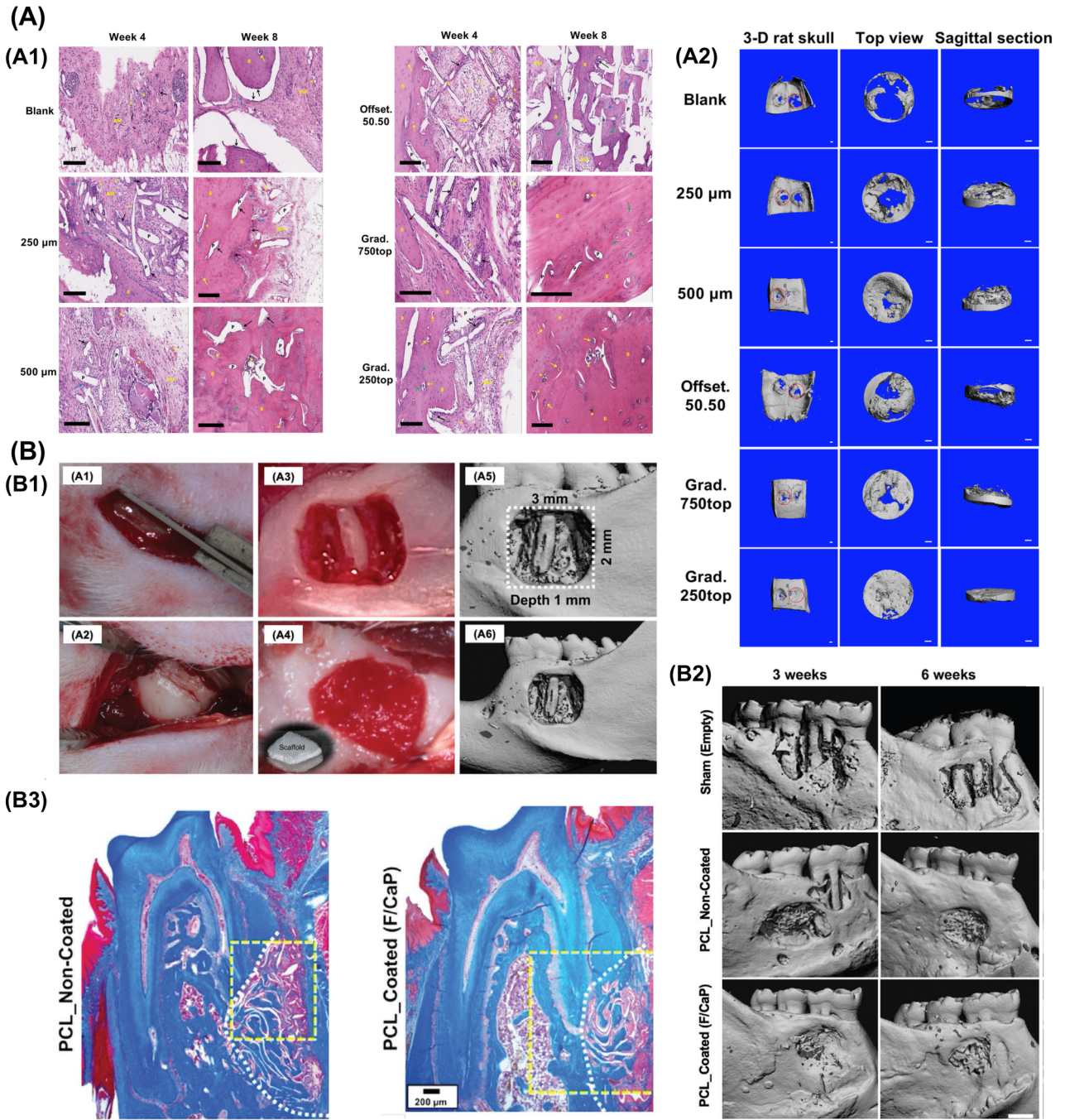


DVG\_23501\_Fig1\_FINAL.tif

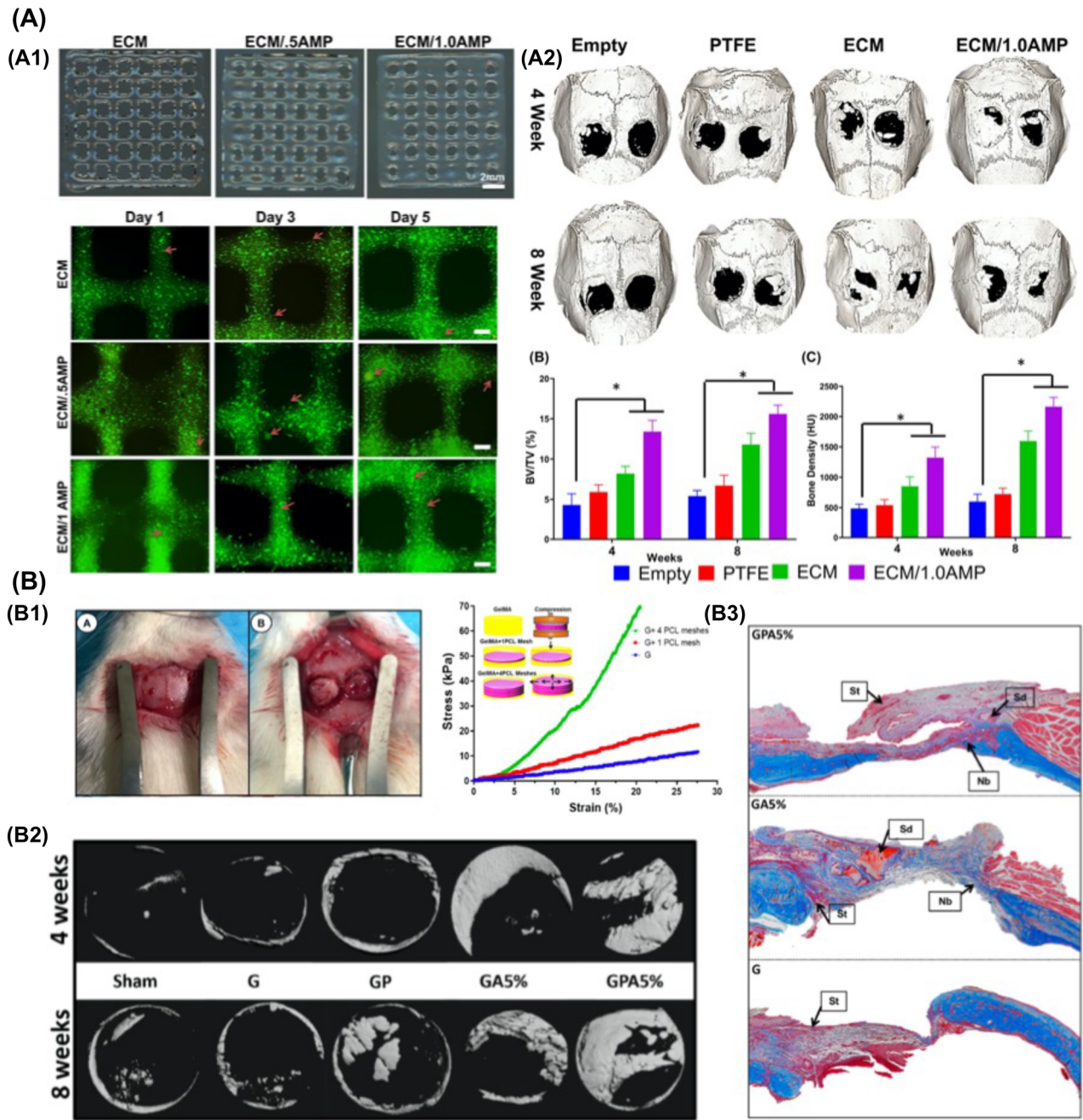




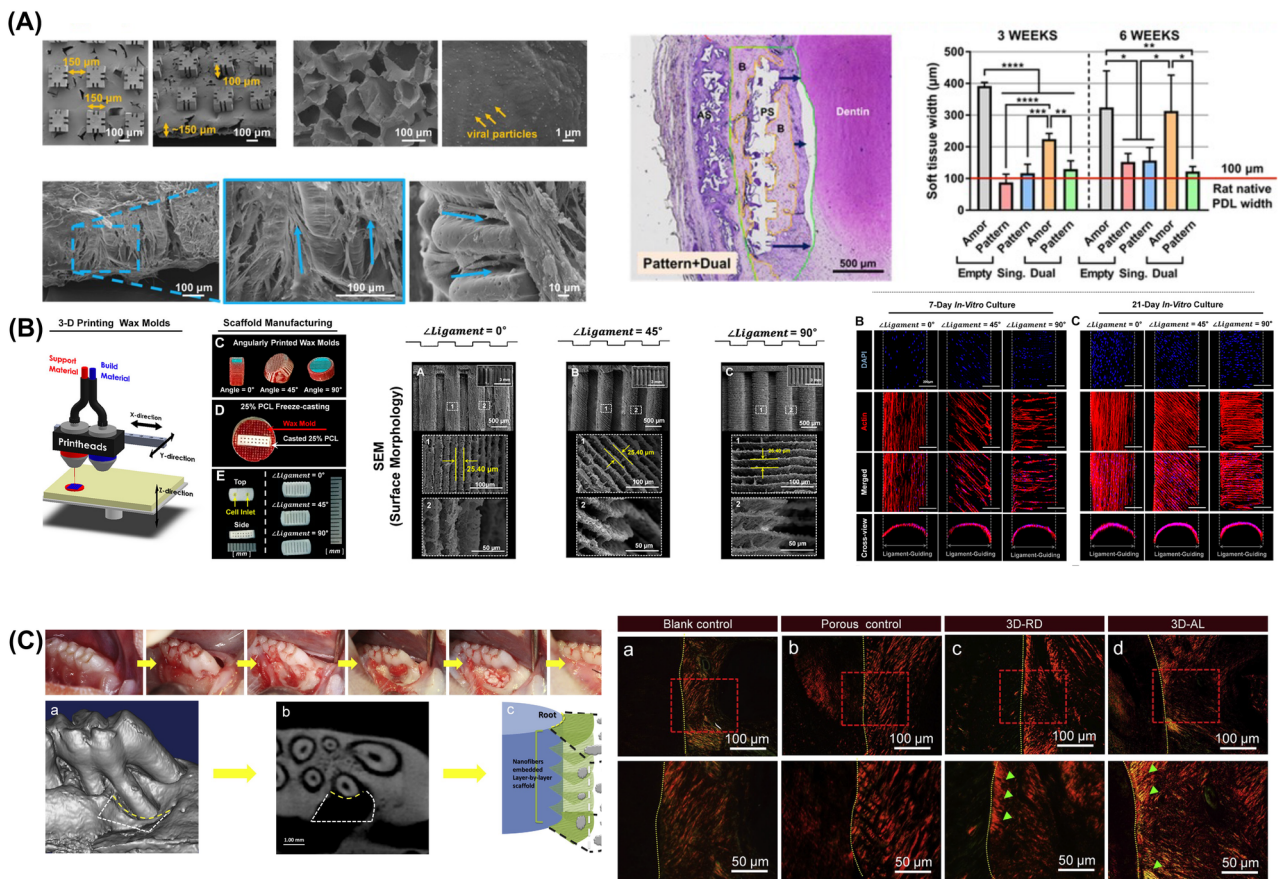
DVG\_23501\_Fig2\_FINAL.tif



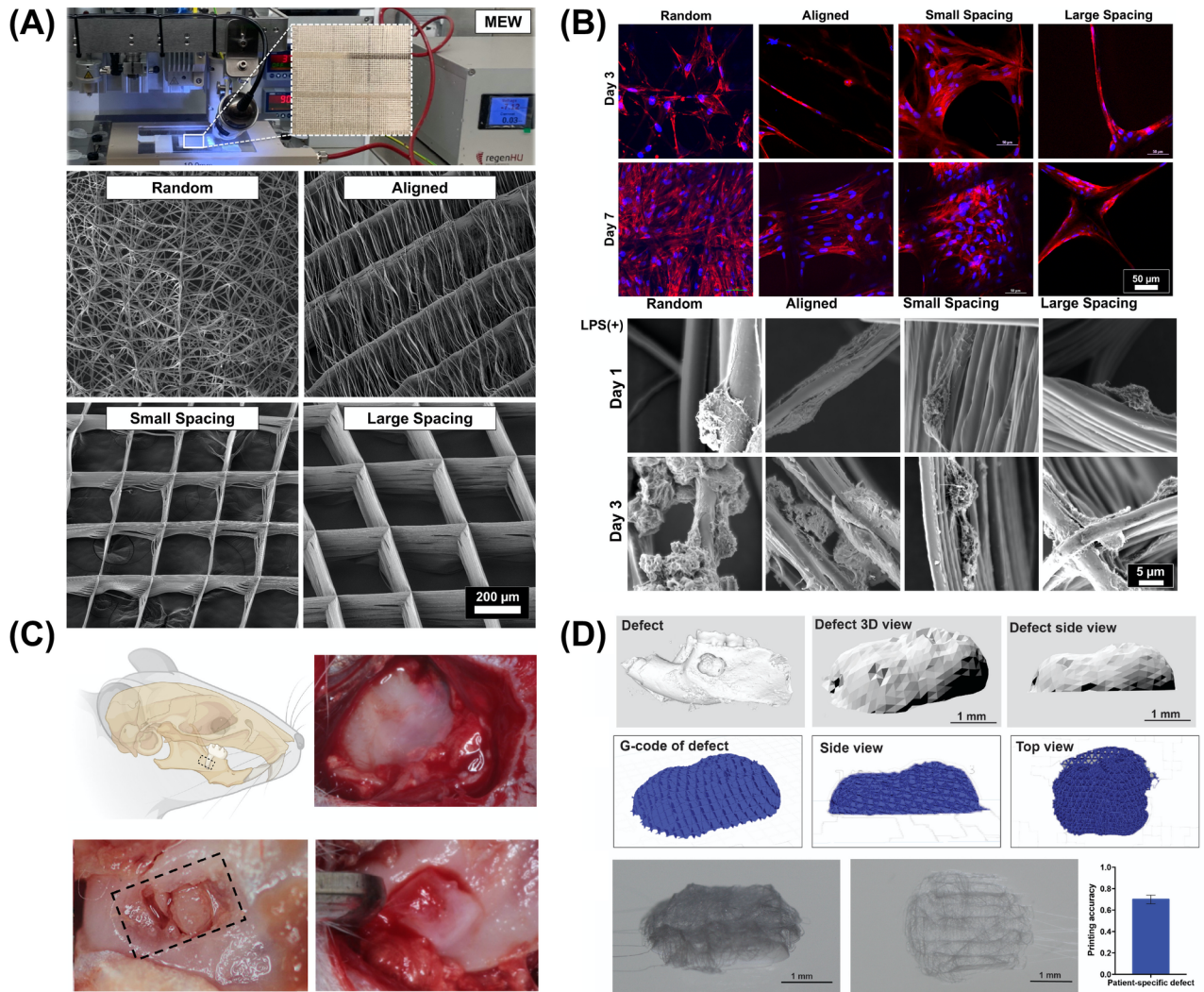
DVG\_23501\_Fig3\_FINAL.tif



DVG\_23501\_Fig4\_FINAL.tif



DVG\_23501\_Fig5\_FINAL.tif



DVG\_23501\_Fig6\_FINAL.tif